JOURNAL OF Applied Polymer SCIENCE

Synthesis, Characterization, and Application of Novel Amphiphilic Poly(D-gluconamidoethyl methacrylate)-*b*-polyurethane-*b*-poly(D-gluconamidoethyl methacrylate) Triblock Copolymers

Niraj Kumar Vishwakarma,[1] Avnish Kumar Mishra,[1] Abhinay Mishra,[2] Tapas Paira,[3] Vijay Kumar Patel,[1] Chandra Sekhar Biswas,[1] Tarun Kumar Mandal,[3] Pralay Maiti,[2] Biswajit Ray[1]

[1]Department of Chemistry, Faculty of Science, Banaras Hindu University, Varanasi 221005, India
[2]School of Material Science and Technology, Institute of Technology, Banaras Hindu University, Varanasi 221005, India
[3]Polymer Science Unit, Indian Association for the Cultivation of Science, Jadavpur, Kolkata 700032, India
Correspondence to: B. Ray (E-mail: biswajitray2003@yahoo.co.in)

ABSTRACT: Novel amphiphilic ABA-type poly(D-gluconamidoethyl methacrylate)-*b*-polyurethane-*b*-poly(D-gluconamidoethyl methacrylate) (PGAMA-*b*-PU-*b*-PGAMA) tri-block copolymers were successfully synthesized via the combination of the step-growth and copper-catalyzed atom transfer radical polymerization (ATRP). Dihydroxy polyurethane (HO-PU-OH) was synthesized by the step-growth polymerization of hexamethylene diisocyanate with poly(tetramethylene glycol). PGAMA-*b*-PU-*b*-PGAMA block copolymers were synthesized via copper-catalyzed ATRP of GAMA in *N*, *N*-dimethyl formamide at 20°C in the presence of 2, 2′-bipyridyl using Br-PU-Br as macroinitiator and characterized by ^{1}H-NMR spectroscopy and GPC. The resulting block copolymer forms spherical micelles in water as observed in TEM study, and also supported by ^{1}H NMR spectroscopy and light scattering. Miceller size increases with increase in hydrophilic PGAMA chain length as revealed by DLS study. The critical micellar concentration values of the resulting block copolymers increased with the increase of the chain length of the PGAMA block. Thermal properties of these block copolymers were studied by thermo-gravimetric analysis, and differential scanning calorimetric study. Spherical Ag-nanoparticles were successfully synthesized using these block copolymers as stabilizer. The dimension of Ag nanoparticle was tailored by altering the chain length of the hydrophilic block of the copolymer. A mechanism has been proposed for the formation of stable and regulated Ag nanoparticle using various chain length of hydrophilic PGAMA block of the tri-block copolymer. © 2012 Wiley Periodicals, Inc. J. Appl. Polym. Sci. 000: 000–000, 2012

KEYWORDS: poly(D-gluconamidoethyl methacrylate)-*b*-polyurethane-*b*-poly(D-gluconamidoethyl methacrylate); critical micellar concentration (CMC); silver nanoparticles

Received 8 June 2012; accepted 30 June 2012; published online
DOI: 10.1002/app.38279

INTRODUCTION

Synthesis of amphiphilic block copolymers using controlled radical polymerization (CRP) technique[1,2] has recently received extensive impetus owing to the prospective application of these block copolymers in drug delivery,[3] coatings,[4–7] nanoparticle synthesis,[8–10] colloidal stabilization,[11–13] and as compatibliser[14–16] for polymer blends. In this respect, amphiphilic block copolymers containing a hydrophilic biocompatible segment made from glycomonomer (sugar containing vinyl monomer) will be of immense interest from the biomedical application point of view owing to its high water solubility, low toxicity,[17] biocompatibility,[17] and bio-conjugation[18,19] properties. Such glycomonomers generally undergo uncontrolled polymerization using conventional radical polymerization. CRP methods such as atom transfer radical polymerization (ATRP), reversible addition-fragmentation chain-transfer polymerization (RAFT) methods were reported for the controlled synthesis of glycopolymers from both protected and unprotected glycomonomers.[20–27] On the other hand, amphiphilic block copolymer containing a hydrophobic polyurethane (PU) segment will be very interesting from the point of its pharmaceutical and biomedical applications owing to its biocompatibility[28,29] and biodegradability.[30] PU can be synthesized using step-growth polymerization method. Reports of the synthesis of tri-block copolymers using different polyurethane-based macroinitiators by CRP techniques were very few in the literature.[31–34] Verma and Kannan reported the synthesis and characterization of polystyrene-*b*-PU-*b*-polystyrene triblock copolymers using step-growth and ATRP polymerization methods.[31] They also reported the synthesis and characterization of

Additional Supporting Information may be found in the online version of this article.

Applied Polymer SCIENCE

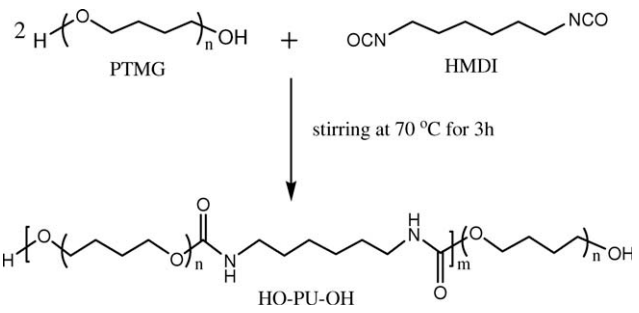

Scheme 1. Synthesis of HO-PU-OH by condensation polymerization method.

poly(methyl methacrylate)-*b*-PU-*b*- poly(methyl methacrylate) triblock copolymers using similar methods.[32] They also reported the synthesis and characterization of poly(methyl methacrylate)-*b*-PU-*b*-poly(methyl methacrylate) triblock copolymers using reverse ATRP method.[33] Schacht et al. reported the synthesis and characterization amphiphilic thermoplastic polyurethane prepared from Pluronic type polyether diols.[34] Recently, Kannan et al. reported the synthesis and characterization of amphiphilic ABA type block copolymer poly(2-(dimethylamino)ethylmethacrylate)-*b*-PU-*b*-poly(2-(dimethylamino)ethylmethacrylate) via the combination of step-growth and ATRP polymerization methods.[35] So far, to our knowledge, the report of the synthesis of amphiphilic block copolymers containing hydrophobic PU segment and hydrophilic glycomonomer segment is not known. Such type of block copolymers may find applications in biomedical field, nanoparticle synthesis fields etc. Here, we report for the first time the synthesis of novel amphiphilic ABA-type tri-block copolymer poly (*D*-Gluconamidoethyl methacrylate)-*b*-PU-*b*-poly (*D*-Gluconamidoethyl methacrylate) (PGAMA-*b*-PU-*b*-PGAMA) by combining the step-growth and ATRP polymerization methods. First, dihydroxy PU (HO-PU-OH) was synthesized by the step-growth polymerization of hexamethylene diisocyanate (HMDI) with poly (tetramethylene glycol) (PTMG) (Scheme 1). Then, the –OH end groups were converted into the corresponding –Br end groups (Br-PU-Br) through the reaction with 2-bromo isobutyryl bromide (Scheme 2). Copper-catalyzed ATRP of GAMA in the presence of 2, 2′-bipyridyl (bpy) ligand in *N*, *N*-dimethyl formamide (DMF) at 20°C was performed to synthesize amphiphilic ABA-type tri-block copolymers PGAMA-*b*-PU-*b*-PGAMA using Br-PU-Br as macroinitiator. The self-assembly behaviors of the resulted block copolymers were studied using

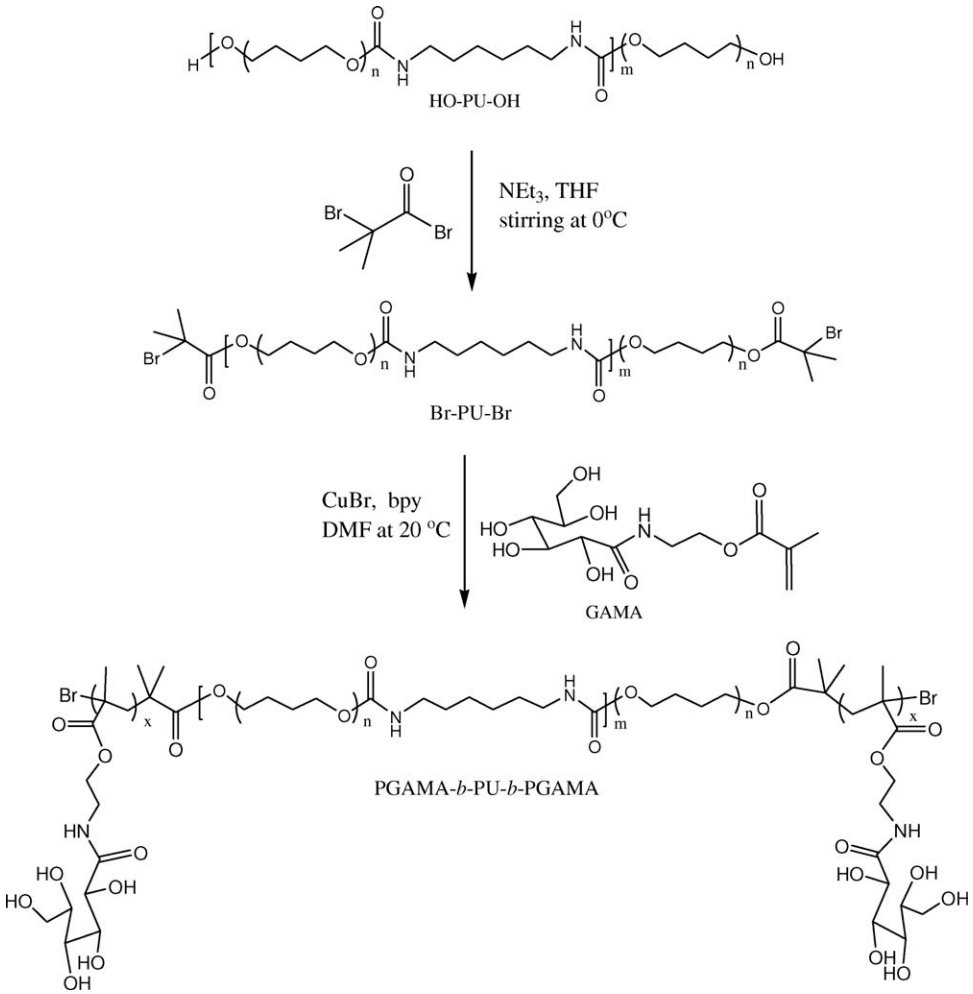

Scheme 2. Synthesis of PGAMA-*b*-PU-*b*-PGAMA block copolymer by copper catalyzed atom transfer radical polymerization method.

Table I. Synthesis of PGAMA-PU-PGAMA Triblock Copolymer[a]

Run	Polymer	GAMA[b] (equiv.)	Time (h)	Convn.[c] (%)	$\bar{M}_n$[d] (theor.)	$\bar{M}_n$[e] (NMR)	$\bar{M}_n$[f] (GPC)	PDI[f]	X_{GAMA}[g] (NMR)	X_{GAMA}[g] (GPC)	CMC[h] (mg/ml)	T_g[i] (°C)	T_m (°C) (PTMG/HMDI)	ΔH_m (J/g) (PTMG/HMDI)
1	HO-PU-OH	-	3	-	-	2680	3300	1.39	-	-	-	−40.9	17.7/97.2	32.5/1.2
2	Br-PU-Br[j]	-	12	88	-	2900	4900	1.37	-	-	-	-	-	
3	$PGAMA_6$-PU-$PGAMA_6$	12	24	100	6584	-	31,700	1.18	0.83	0.84	0.012	88.7	9.6/88.3	
4	$PGAMA_{15}$-PU-$PGAMA_{15}$	30	43	100	12,110	-	74,700	1.73	0.92	0.93	0.039	88.4	-	
5	$PGAMA_{30}$-PU-$PGAMA_{30}$	60	45	100	21,320	-	127,600	1.84	0.97	0.96	0.090	86.3	-	

[a]Using Br-PU-Br : CuBr : bpy :: 1 : 2 : 4 in DMF at 20°C, [b]GAMA equivalent taken with respect to Br-PU-Br, [c]Monomer conversion determined by ^{1}HNMR in DMSO-d_6, [d]$\bar{M}_n(\text{theor}) = \frac{[\text{GAMA}]_o}{[\text{Br-PU-Br}]_o} \cdot X_{GAMA} \cdot M_{GAMA} + M_{\text{Br-PU-Br(NMR)}}$, [e]Determined by ^{1}HNMR, [f]Determined by Gel Permeation chromatography (DMF, 1.0 mL/min at 40°C and calibrated against PMMA standard), [g]Composition of GAMA in block copolymer determined by ^{1}HNMR and GPC, [h]Critical micelle concentration (CMC) determined by fluoroscence spectrometry using pyrene as probe, [i]T_g of PGAMA is observed at 85.5°C, [j]Br-PU-Br synthesisd by HO-PU-OH : 2-bromoisobutyryl bromide :: 1 : 2.5.

^{1}H-NMR, TEM, and fluorescence spectroscopy. Thermal properties of these block copolymers were studied by TGA and DSC. Moreover, Ag-nanoparticles were synthesized using these block copolymers as colloidal stabilizer.

EXPERIMENTAL

Materials

D-Gluconolactone (Fluka, Ireland, 99%), 2-aminoethylmethacrylate hydrochloride (Aldrich, St Louis, MO, 90%), 2-bromoisobutyryl bromide (Aldrich, Steinheim, Germany, 98%), hexamethylene diisocyanate (HMDI) (Aldrich, St Louis, MO, 98%) and polytetramethylene glycol (M_n = 1400) (PTMG) (Aldrich, St Louis, MO) were used as received. *D*-Gluconamidoethyl methacrylate (GAMA) was synthesized following the procedure as reported in the literature.[27] Cuprous bromide (Aldrich, Steinheim, Germany, 98%) was purified using a reported procedure[36] and dried under vacuum. 2, 2′-Bipyridyl (Qualigens, Mumbai, India, 99.5%), sodium hydrogen carbonate (Loba Chemie, Mumbai, India, 99.5%), anhydrous magnesium sulfate (Loba Chemie, Mumbai, India, extra pure) were used as received. *N, N*-Dimethyl formamide (DMF) (Spectrochem, Mumbai, India, 99.5%) was distilled over anhydrous magnesium sulfate. Methanol (Loba Chemie, Mumbai, India, 99%) and isopropanol (Loba Chemie, Mumbai, India, 99%) were dried and distilled over anhydrous calcium oxide. Tetrahydrofuran (Loba Chemie, Mumbai, India, 99%) was dried and fractionally distilled over sodium wire in the presence of benzophenone. Deionized water was prepared by redistillation of the double distilled water in an all-glass distillation apparatus.

General Methods

^{1}H-NMR spectra were recorded on a JEOL AL300 FTNMR (300 MHz) at ambient temperature in $CDCl_3$ or D_2O or DMSO-d_6 as solvent, and are reported in parts per million (δ) from internal standard tetramethylsilane or residual solvent peak. GAMA monomer conversion (%) was determined using ^{1}H NMR in D_2O or DMSO-d_6 by comparing the integrated peak area of the residual vinylic signals at 5.0–6.0 ppm (2H) of the monomer with that of the backbone α-methyl peak at 0.5–1.2 ppm (3H) of the corresponding polymer. FTIR spectra of the dried polymers were taken in the 400–4000 cm^{-1} range by making the pellet with KBr. The number average molecular weight (M_n) and polydispersity index (M_w/M_n) were determined by Younglin ACME 9000 Gel Permeation Chromatography in DMF at 40°C with flow rate 1.0 mL/min on two polystyrene gel columns [PL gel 5 μm 10E 4 Å columns (300 × 7.5 mm)] connected in series to Younglin ACME 9000 Pump and a Younglin ACME 9000 RI detector. The columns were calibrated against seven poly (methyl methacrylate) (PMMA) standard samples (Polymer Lab, PMMA Calibration Kit, M-M-10). The theoretical number average molecular weight [M_n (theor)] of the resulted PGAMA-*b*-PU-*b*-PGAMA block polymer using Br-PU-Br macroinitiator was calculated using the following equation:

$$\bar{M}_n(\text{theor}) = \frac{[\text{GAMA}]_o}{[\text{Br} - \text{PU} - \text{Br}]_o} \cdot x_{\text{GAMA}} \cdot M_{\text{GAMA}} + M_{\text{Br-PU-Br}}\,(\text{NMR})$$

where x_{GAMA} is the fraction conversion of monomer, M_{GAMA} is the molecular weight of monomer and $M_{\text{Br-PU-Br}}$ (NMR) is the

molecular weight of the Br-PU-Br macroinitiator determined from its ^{1}H-NMR. The UV-visible absorption spectra of as-prepared Ag nanoparticle solutions were recorded using a JASCO V-670 UV-Visible spectrophotometer at room temperature. TEM images were obtained using JEOL, JEM, 2100 transmission electron microscopes operating at an acceleration voltage of 200 kV. For TEM measurement of the aqueous block copolymer solution (0.5 mg/mL), samples were prepared by casting a drop of it on the carbon coated copper grid followed by the removal of extra solution with a filter paper and dried under vacuum at room temperature. For TEM measurement of Ag colloids, samples were prepared by casting a drop of the appropriately diluted dispersion on to the carbon coated copper grid followed by the soaking of the excess solvent using a wet blotting paper, and dried under vacuum at room temperature.

Fluorescence Experiments

Fluorescence measurements were carried out on a Varian Cary Eclipse Fluorescence Spectrometer using a series of aqueous PGAMA-*b*-PU-*b*-PGAMA triblock copolymer solutions with concentrations ranging from 1×10^{-4} to 1 mg/mL having pyrene concentration of $6 \times 10^{-7}M$. Details of the experimental procedure were given elsewhere.[37]

Light Scattering Experiments

DLS experiments of block copolymers and silver nanoparticles were carried out by a Brookhaven laser scattering system[37] equipped with a BI-200SM research goniometer, a TurboCorr digital corrector (BI-9000AT) with a maximum number of 522 channels, and a He–Ne laser of a wavelength 632.8 nm was used. Solutions were filtered by a nylon 6,6 filter paper of 0.45 μm pour diameter to remove dust particle. The particle size distributions were performed at 25°C at a fixed scattering angle of 90°. Details of the experimental procedure were given elsewhere.[37]

Thermal Study

Thermo gravimetric analysis (TGA) was performed using Mettler TGA thermo gravimetric analyzer in the temperature range from 40 to 600°C with a heating rate of 20°C/min under N_2 atmosphere. Differential Scanning Calorimeter (DSC) measurement was performed using Mettler 832 DSC instrument under N_2 atmosphere. The instrument is calibrated with indium before use. The samples were first heated to 200°C at 20°C/min heating rate and held at this temperature for 5 min to remove the thermal history, followed by quenching to −120°C. A heating rate of 10°C/min was used for second heating run. Results were reported from the second heating run. The glass transition temperature (T_g) was taken as the midpoint of the heat capacity change. The melting temperature (T_m) was taken as the temperature of maximum of endothermic peak.

Synthesis of Hydroxyl-Terminated Polyurethanes (HO-PU-OH) (Scheme 1) (Run 1, Table I)

In a 150 mL dried and nitrogen purged round-bottom flask, polytetramethylene glycol (PTMG, M_n = 1400 g mol^{-1}) (5 g, 3.57 mmol) was taken and melted at 70°C. To it, 1, 6-hexamethylene diisocyanate (HMDI) (0.3004 g, 1.79 mmol) was added with stirring under nitrogen atmosphere at 70°C, and stirring was continued for 3h at 70°C. A paste-like white product, which was solid at room temperature, was formed. Yield (gravimetric) = 96%. ^{1}H-NMR ($CDCl_3$, 300 MHz) [Figure 1(a)]: δ = 1.31 (b, $4H_i$), 1.45 (b, $4H_h$), 1.62 (s, $4H_b + 8H_c + 4H_e$), 2.55 (t, $2H_j$), 3.18 (t, $4H_g$), 3.41 (s, $16H_d$), 3.62 (t, $4H_a$), 4.05 (t, $4H_f$). M_n (NMR) = 2680 g mol^{-1}, M_n (GPC) = 3300 g mol^{-1}, M_w/M_n = 1.39.

Synthesis of Polyurethanes Dibromide (Br-PU-Br) (Scheme 2) (Run 2, Table I)

In a 100 mL dried and nitrogen purged round-bottomed flask, polyurethane dihydroxy [M_n (NMR) = 2680 g mol^{-1}, 2 g, 7.46×10^{-4} mol] was dissolved in dry THF (40 mL) with triethylamine (0.73 mL, 5.25 mmol) with stirring under N_2 atmosphere. Then, 2-bromoisobutyryl bromide (0.35 mL, 2.83 mmol) was added dropwise to the above-mentioned reaction mixture that was cooled in an ice bath. The reaction mixture was then stirred overnight at room temperature. The precipitated by-product (i.e., $Et_3N.HBr$) was removed by filtration and the filtrate was evaporated to dryness. The resulting yellow oil was dissolved in dichloromethane (40 mL) and washed thoroughly with saturated aqueous sodium hydrogen carbonate solution (3 × 50 mL). The organic layer was further washed with water (3 × 100 mL), dried over anhydrous magnesium sulfate, filtered. The filtrate was evaporated and dried under vacuum at room temperature to get the yellow paste product. Yield (gravimetric) = ∼100%. ^{1}H-NMR (300 MHz, $CDCl_3$) [Figure 1(b)]: δ = 1.31 (b, $4H_i$), 1.45 (b, $4H_h$), 1.62 (s, $4H_b + 8H_c + 4H_e$), 1.85 (s, $12H_k$), 3.18 (t, $4H_g$), 3.41 (s, $16H_d$), 4.05 (t, $4H_f$), 4.2 (t, $4H_a$). M_n (NMR) = 2900 g mol^{-1}, M_n (GPC) = 4900 g mol^{-1}, M_w/M_n = 1.37.

Typical Synthesis of PGAMA$_6$-*b*-PU-*b*-PGAMA$_6$ Triblock Copolymer (Scheme 2) (Run 3, Table I)

In a dried and nitrogen purged Schlenk tube, 0.1 g [3.45×10^{-5} mol, calculated on the basis of molecular weight (2900 g mol^{-1}) obtained from ^{1}H NMR] Br-PU-Br was dissolved in 1 mL of DMF. To it, 125 mg (4.07×10^{-4} mol) GAMA and 5.9 mg (4.1×10^{-5} mol) CuBr were added. A homogeneous solution was obtained after stirring and degassed under nitrogen for 30 min. A stock solution of 2, 2′ bipyridyl in DMF was prepared beforehand having concentration of 16.4×10^{-2} mol/L and purged with nitrogen for 30 min. Totally, 0.5 mL (containing 12.8 mg, 8.2×10^{-5} mol) of this nitrogen-purged bipyridyl solution was added under nitrogen atmosphere to the above-mentioned reaction mixture that was maintained at 20°C. The reaction was continued at 20°C for 24 h. The reaction was stopped by freezing the reaction mixture with liquid nitrogen, and exposed to the air. A small portion of the polymerization mixture was used to determine the monomer conversion by ^{1}H-NMR. Observed monomer conversion by ^{1}H-NMR was 100%. The rest of the polymerization mixture was passed through a basic alumina column using DMF/water mixture (1:1, v/v) as eluent to remove ATRP catalyst. The filtrate was concentrated, and precipitated into 75 mL methanol, and dried under vacuum at room temperature for 24 h.

^{1}H-NMR (300 MHz, DMSO-d_6): δ (ppm) = 0.5–1.2 (b, $6H_m$), 1.21 (s, $4H_i + 12H_k$), 1.46 (s, $16H_c + 4H_e + 4H_h$), 1.76 (b, $4H_b + 4H_l$), 3.19 (t, $4H_g$), 3.43–3.69 (b, $16H_d + 2H_s + 2H_t +$

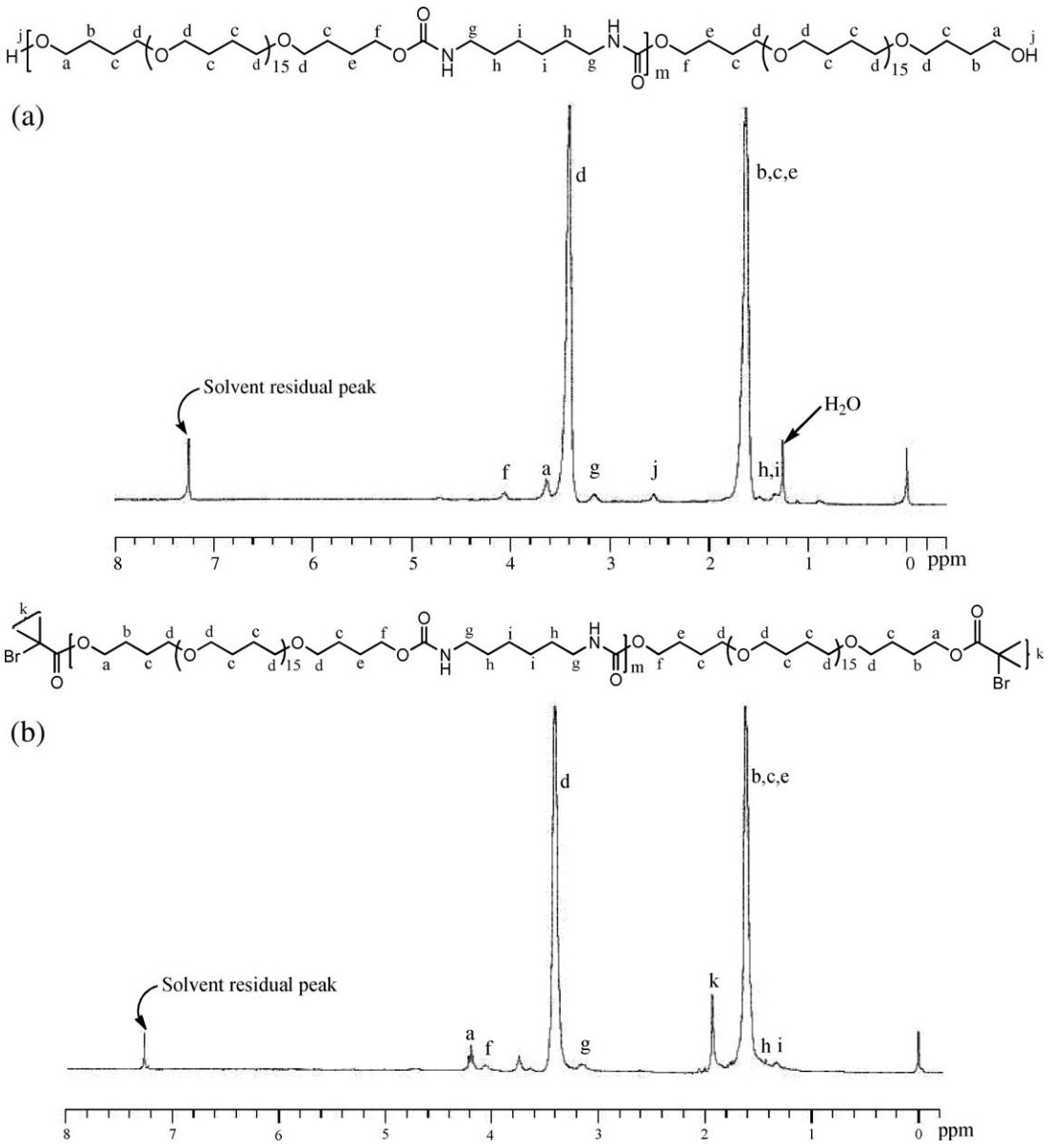

Figure 1. (a) ^{1}H NMR spectrum of HO-PU-OH in *d*-chloroform at ambient temperature. (b) ^{1}H-NMR spectrum of Br-PU-Br in *d*-chloroform at ambient temperature.

$4H_u$), 3.75–4.23 (b, $4H_a + 4H_o$), 4.3–4.75 (b, $4H_f + 4H_n + 2H_q + 2H_r$), 5.38 (s, $2H_p$).

$M_n(\text{GPC}) = 31,700$ g mol^{-1}, $M_w/M_n = 1.18$.

Synthesis of Silver Nanoparticles

The block copolymer $PGAMA_{30}$-*b*-PU-*b*-$PGAMA_{30}$ (32 mg, 2.09×10^{-5} mol/L) (run 5, Table I) was dissolved in 12 mL deionized water/DMF (9:1, v/v) mixture. The solution was sonicated for 1 h. To it, under stirring, 0.3 mL of 0.03*M* aqueous $AgNO_3$ solution was added followed by the addition of 0.3 mL 0.03*M* $NaBH_4$ solution. Stirring of the reaction mixture was continued for 1 h at 30°C. A reddish brown colored transparent solution was finally formed, which was stable even after 1 year. A blank reaction was also carried out simultaneously without using block copolymer.

RESULTS AND DISCUSSION

Synthesis of PGAMA-*b*-PU-*b*-PGAMA Triblock Copolymers

A new amphiphilic triblock copolymer PGAMA-*b*-PU-*b*-PGAMA was synthesized via the combination of condensation polymerization and copper-catalyzed atom transfer radical polymerization. In the first step, HO-PU-OH was synthesized via condensation polymerization of PTMG and HMDI (2.1:1 molar ratio) in molten condition at 70°C (Scheme 1). Figure 1(a) shows the ^{1}H-NMR of the resulting polymer. The characteristics peaks at ~3.41 ppm (d) and ~1.63 ppm (b, c, e) correspond to the aliphatic methylene protons of the backbone PU chain and

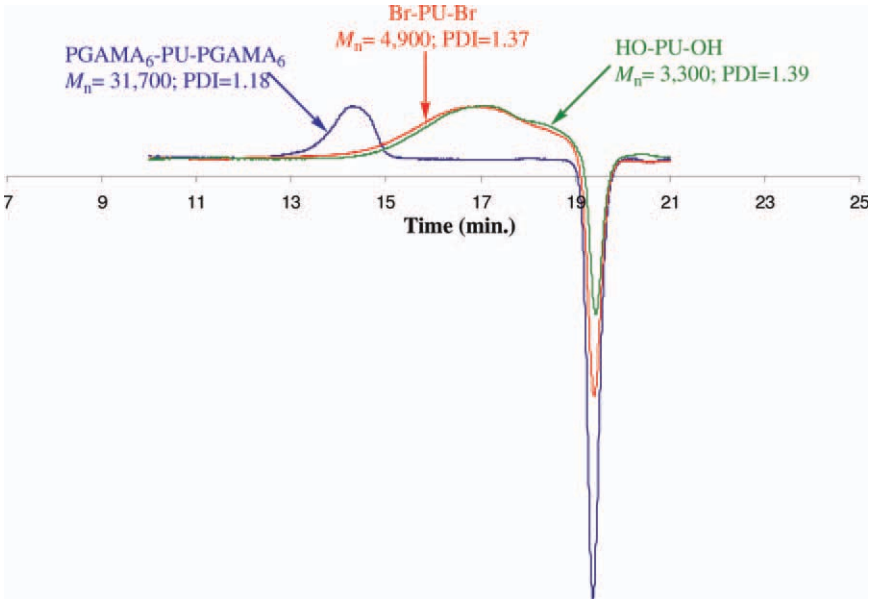

Figure 2. Gel permeation chromatograms of HO-PU-OH, Br-PU-Br, and PGAMA$_6$-*b*-PU-*b*-PGAMA$_6$ at 40°C in DMF. [Color figure can be viewed in the online issue, which is available at wileyonlinelibrary.com.]

the peak at ~2.55 ppm corresponds to the hydroxyl proton (j) of the polymer chain-end.

The number average molecular weight of this polymer calculated from its ^{1}H-NMR, [M_n (NMR)] [*vide* Figure 1(a)] by comparing the peak area of the aliphatic methylene protons of the backbone PU chain at ~3.41 ppm (d) to that of the hydroxyl proton (j) of the polymer chain-end at ~2.55 ppm was found to be 2680 g mol^{-1}. The corresponding observed number average molecular weight [M_n (GPC)] and its distribution (PDI) determined by GPC were 3300 g mol^{-1}, and 1.39, respectively (run 1, Table I and Figure 2). The observed difference in molecular weights determined by ^{1}H-NMR [M_n (NMR)] and GPC [M_n (GPC)] is due to the use of PMMA standards for calibration in the analysis of the GPC method. The presence of a hump at the lower molecular weight part of the corresponding chromatogram indicates the presence of PTMG as an impurity of 7–8% calculated by the deconvolution of the chromatogram. HO-PU-OH was reacted with 2-bromoisobutyryl bromide in the presence of triethylamine to prepare 2- bromoisobutyryl-terminated PU (Br-PU-Br) (Scheme 2) (run 2, Table I). Figure 1(b) shows the ^{1}H-NMR of the corresponding polymer. The incorporation of the 2-bromoisobutyryl groups at the polymer chain-end was confirmed from the appearance of methyl (k) protons of 2-bromopisobutyryl end-group of the resulting polymer at around 1.85 ppm. The observed conversion (%) of the –OH into its corresponding 2-bromoisobutyryl end-group calculated using ^{1}H NMR by comparing the peak area of the hydroxyl proton at ~2.55 ppm with that of the methyl protons of 2-bromoisobutyryl end-group at ~1.85 ppm was around 88%. The observed M_n (NMR) of this polymer calculated from its ^{1}H-NMR [Figure 1(b)] by comparing the peak area of the aliphatic methylene protons of the backbone PU chain at ~3.41 ppm (d) to that of the methylene protons (a) of the polymer chain-end at ~4.2 ppm was 2900 g mol^{-1}. The corresponding observed M_n (GPC) and PDI were 4900 g mol^{-1} and 1.37, respectively (run 2, Table I and Figure 2). The observed higher value of M_n (GPC) of Br-PU-Br with respect to that of HO-PU-OH is due to change in the hydrodynamic volume owing to the incorporation of 2-bromoisobutyryl end-group.

The Br-PU-Br was then used as macroinitiator for the copper-catalyzed ATRP of GAMA in DMF using [Br-PU-Br]: [CuBr]: [bpy] = 1: 2: 4 at 20°C (Table I). Runs 3, 4, and 5 (Table I) correspond to 12, 30, and 60 equivalent of GAMA monomer loading with respect to the Br-PU-Br macroinitiator, respectively. The corresponding monomer conversions were about 100%. Molecular weight of the corresponding block copolymers increased with increase in the monomer loading as expected. Typical GPC chromatograms of run 3 (Figure 2) show the shift of the polymer peak toward higher molecular weight. Moreover, typical ^{1}H-NMR spectrum of the block copolymer (run 5) in DMSO-d_6 [Figure 3(a)] shows, in addition to the characteristic peaks of the PU block, the presence of the characteristic peaks of the backbone methylene protons (l) at ~ 1.55–2.15 ppm, and the backbone methyl protons (m) of the PGAMA block at ~0.5–1.2 ppm apart from other methylene and methine protons of the PGAMA block overlapped at ~3.75–4.23 and ~4.3–4.75 ppm. The observed mole-fraction of PGAMA block in these block copolymers calculated on the basis of ^{1}H-NMR and GPC molecular weights were within the range of 0.83–0.97. The observed difference in different molecular weights is (1) due to the change in the hydrodynamic volume owing to the incorporation of PGAMA block in the corresponding block copolymer, and (2) due to the use of standard PMMA polymers for calibration in GPC method.

Therefore, the synthesis of these block copolymers confirms the successful occurrence of the chain extensions.

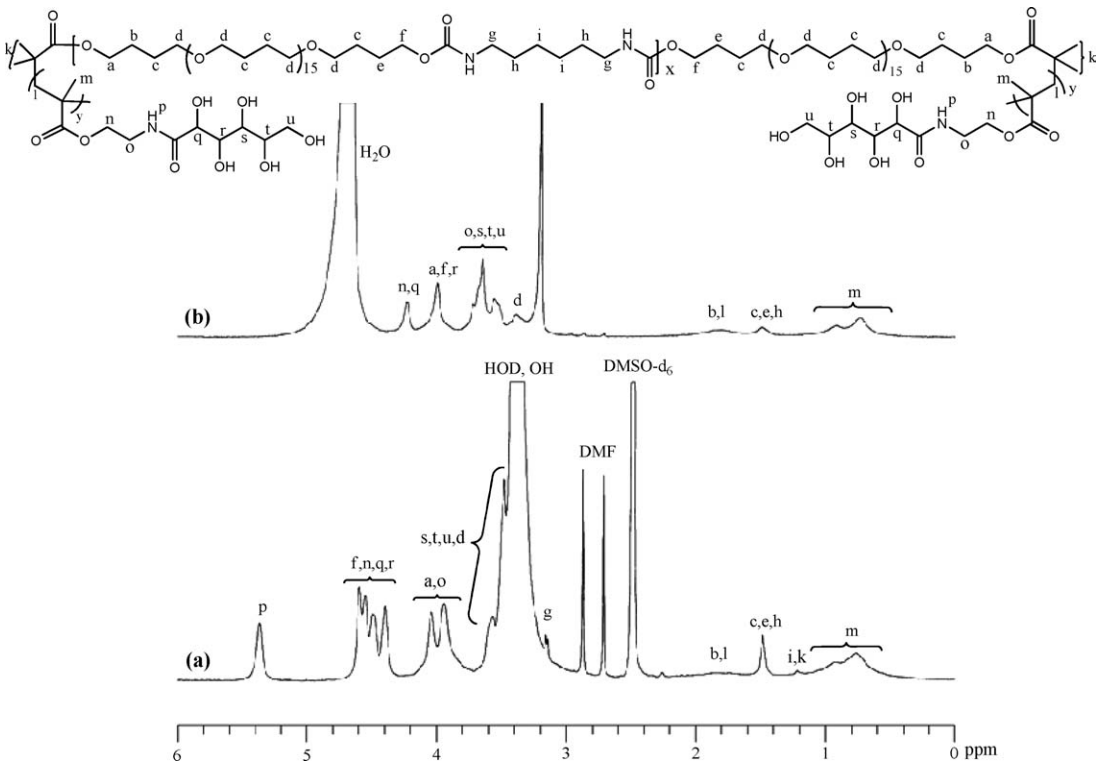

Figure 3. ^{1}H-NMR spectra of triblock copolymer of PGAMA$_{30}$-*b*-PU-*b*-PGAMA$_{30}$ in DMSO-d_6 (a) and D_2O (b) at ambient temperature.

FTIR Studies

Figure 4 shows the FTIR spectra of (a) HO-PU-OH, (b) Br-PU-Br, and (c) triblock copolymer PGAMA$_{30}$-*b*-PU-*b*-PGAMA$_{30}$. In all spectra, the band at 2850–2940 cm^{-1} corresponds to both the symmetric and asymmetric C—H stretching vibrations. The single stretching vibration of the polyurethane carbonyl (C=O) group was observed at around 1717 and 1733 cm^{-1} in HO-PU-OH and Br-PU-Br, respectively; but, in the block copolymer, two stretching vibrations of the carbonyl (C=O) groups were observed at 1725 and 1657 cm^{-1} : first one was due to the urethane (NH(C=O)O) linkage in polyurethane chain as well as due to the ester linkage in PGAMA chain and second one was due to the amide (NHC=O) linkage in PGAMA chain. The C=O stretching frequency of PGAMA was observed at 1719 and 1652 cm^{-1} (Supporting Information).

The shifting of peak positions clearly indicates block copolymer formation and change in interaction. Moreover, the broad band at 3466 cm^{-1} in HO-PU-OH was due to the presence of the N—H and the O—H stretching vibrations, while the low intensity band at 3346 cm^{-1} in Br-PU-Br was due to the N—H stretching vibrations alone. The observed low intensity of this band supports the formation of bromo substituted PU. On the other hand, a high intensity broad band was observed at 3415 cm^{-1} in the block copolymer due to the combined N—H stretching vibrations in PU chain and the O—H stretching vibrations in PGAMA chain. Observation of all these bands clearly supports the formation of triblock copolymer. In addition to these, the C—H bending vibrations of methylene groups were observed at 1446, 1460, and 1444 cm^{-1} in HO-PU-OH, Br-PU-Br, and the block copolymer, respectively; stretching vibrations of the O—C bond adjacent to the ester linkages were observed at 1112, 1162, and 1160 cm^{-1} in HO-PU-OH, Br-PU-Br, and block copolymer, respectively. The presence of a new peak at 642 cm^{-1} in Br-PU-Br corresponds to C—Br bond. Presence of all these FTIR bands supports the formation of Br-PU-Br and PGAMA-*b*-PU-*b*-PGAMA from HO-PU-OH.

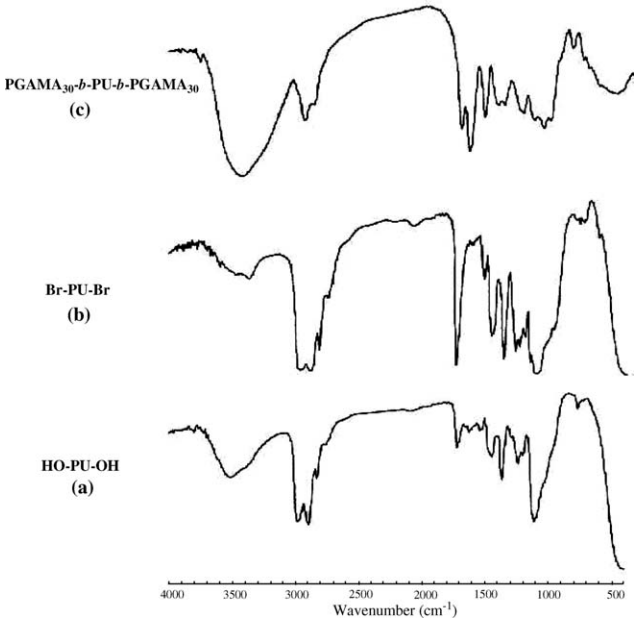

Figure 4. FTIR spectra of (a) HO-PU-OH (b) Br-PU-Br, and (c) PGAMA$_{30}$-*b*-PU-*b*-PGAMA$_{30}$.

Applied Polymer SCIENCE

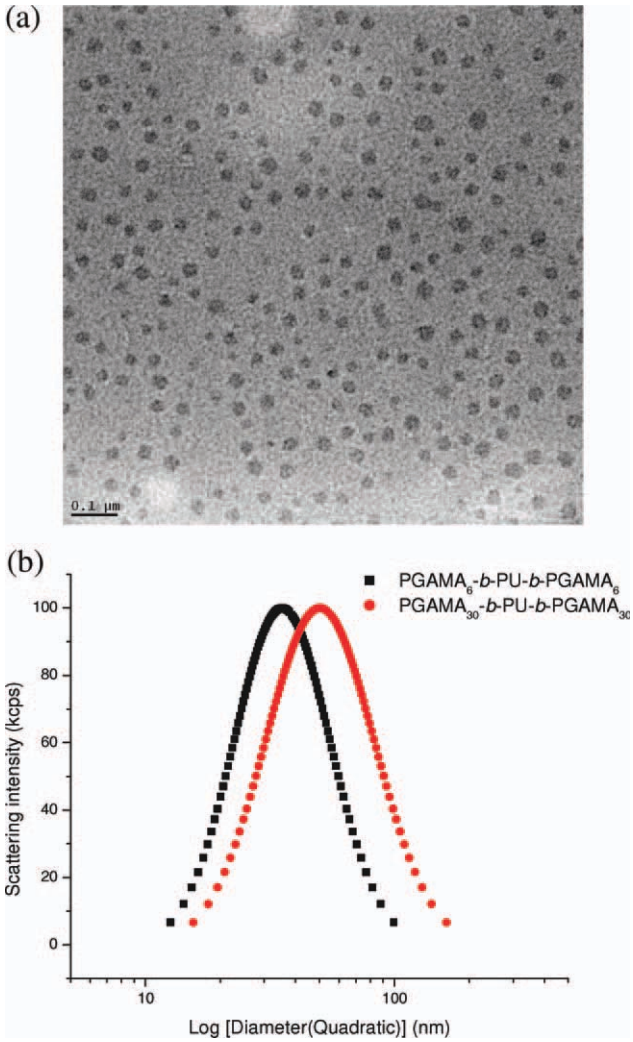

Figure 5. (a) TEM image of the micelles obtained from aqueous solution of $PGAMA_{30}$-*b*-PU-*b*-$PGAMA_{30}$ (run 5, Table I) (0.5 mg/mL). (b) Hydrodynamic diameter (quadratic) distribution/plot of scattering intensity vs. effective hydrodynamic diameter (quadratic) of $PGAMA_6$-*b*-PU-*b*-$PGAMA_6$ and $PGAMA_{30}$-*b*-PU-*b*-$PGAMA_{30}$ at 0.5 mg/mL concentration in water at 90° scattering angle. [Color figure can be viewed in the online issue, which is available at wileyonlinelibrary.com.]

Self-Assembly of Amphiphilic Triblock Copolymer

The ^{1}H-NMR of $PGAMA_{30}$-*b*-PU-*b*-$PGAMA_{30}$ block copolymer in D_2O [Figure 3(b)] clearly shows the suppression of all characteristic peaks of the PU block in contrary to the presence of all characteristic peaks of the PU and the PGAMA blocks in the ^{1}H-NMR of the same in DMSO-d_6 [Figure 3(a)]. This observation indicated the possible formation of micellar aggregates in D_2O with PU-block as the core and PGAMA-block as the shell which was confirmed from the TEM image [Figure 5(a)] of the uniform spherical micelles formed in water with an average micellar dimension of ~35.2 nm. The corresponding observed average miceller diameter obtained from DLS measurement at 90° scattering angle was higher (~50.2 nm) [Figure 5(b) and Supporting Information Figure S1a]. This is presumably due to the collapse of the micellar structure on TEM grids during drying up process.[37] Moreover, Figure 5(b) also shows that miceller diameter decreases with the increase in the hydrophilic PGAMA block length as expected.

To study the critical micellar concentration (CMC) of these block copolymers in water, fluorescence spectroscopy technique was employed with pyrene as probe.[38–40] Figure 6(a) shows the typical fluorescence excitation spectra (300–360 nm) of pyrene ($6 \times 10^{-7} M$) at different $PGAMA_{30}$-*b*-PU-*b*-$PGAMA_{30}$ concentration recorded at an emission wavelength of 394 nm. Figure 6(b) shows the corresponding plot of the ratio of the peak intensities of the excitation spectra of pyrene at 337.07 nm ($I_{337.07}$) and 333.07 nm ($I_{333.07}$) vs. the logarithmic concentration (mg/mL) of the block copolymer in water. The sharp inflection point of two straight lines at lower concentration was considered as the CMC of the block copolymer. The observed CMC was ~0.09 mg/mL (run 5, Table I). CMC values of the block copolymers have increased with the increase of the chain length of the hydrophilic PGAMA block as expected, e.g., 0.012 mg/mL for $PGAMA_6$-*b*-PU-*b*-$PGAMA_6$ and 0.039 mg/mL for $PGAMA_{15}$-*b*-PU-*b*-$PGAMA_{15}$ (runs 3 and 4, Table I, Supporting

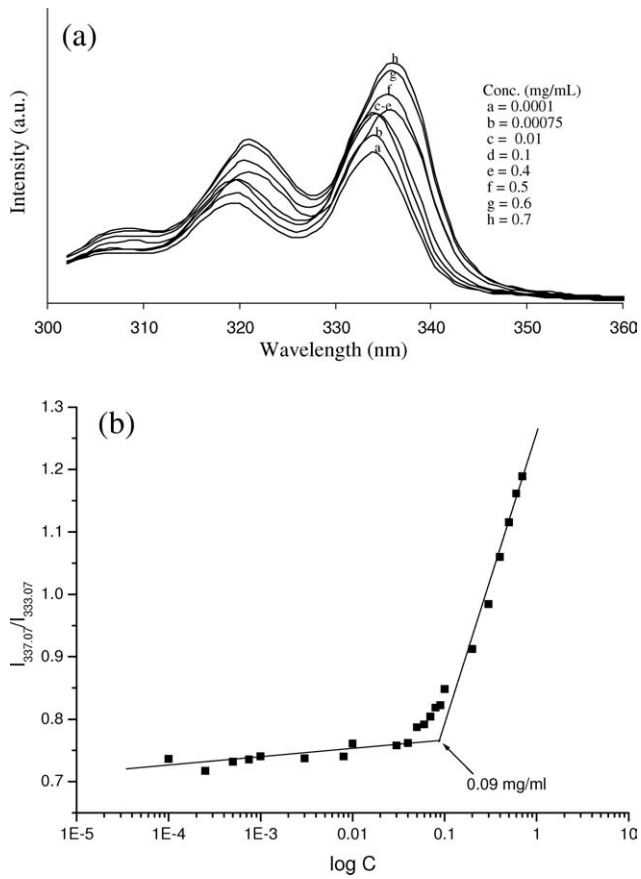

Figure 6. (a) Fluorescence excitation spectra (300–360 nm) (monitored at $\lambda_{em} = 394$ nm) of pyrene ($6 \times 10^{-7} M$) in the presence of increasing concentration (mg/mL) of the block copolymer $PGAMA_{30}$-*b*-PU-*b*-$PGAMA_{30}$ (run 5, Table I) solution in water. (b) Semi-logarithmic plot of the fluorescence excitation intensity ratio ($I_{337.07}/I_{333.07}$) of pyrene ($6 \times 10^{-7} M$) (monitored at $\lambda_{em} = 394$ nm) vs. the concentration (mg/mL) of the block copolymer $PGAMA_{30}$-*b*-PU-*b*-$PGAMA_{30}$ in water.

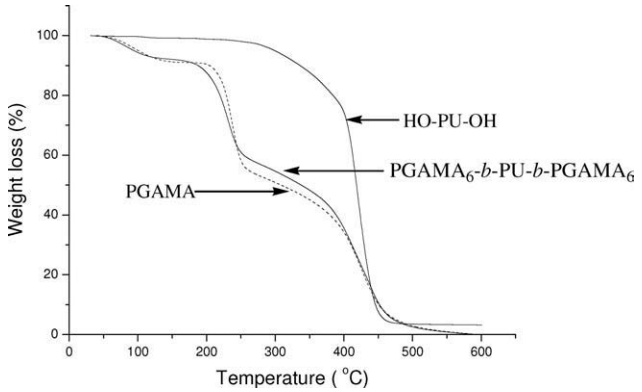

Figure 7. TGA curves of HO-PU-OH, PGAMA, and the triblock copolymer $PGAMA_6$-*b*-PU-*b*-$PGAMA_6$.

Information Figures S2 and S3). Similar types of results for A-B-A type hydrophilic-end amphiphilic triblock copolymer were also reported in the literature.[39] All these observations confirmed the amphiphilic character of the formed PGAMA-*b*-PU-*b*-PGAMA block copolymers.

Thermal Analysis

Figure 7 shows the TGA curves of HO-PU-OH, PGAMA, and the block copolymer $PGAMA_6$-*b*-PU-*b*-$PGAMA_6$ (run 3, Table I). The decomposition of PU occurred through the initial gradual loss in the region ~250–400°C due to the decomposition of urethane linkage followed by the greater mass loss in the region ~ 400−470°C due to the decomposition of PTMG block.[41] Thermal stability of PGAMA was lower than that of PU. $PGAMA_6$-*b*-PU-*b*-$PGAMA_6$ block copolymer undergo initial slight weight loss in the region ~90–120°C owing to the evaporation of adsorbed moisture followed by two stage broad mass losses: one at ~200–250°C region was due to the decomposition of PGAMA and another one at ~250−550°C region was due to the decomposition of PU chains. Profiles of the TGA curves of the block copolymers were close to that of PGAMA due to the presence of two blocks of PGAMA in the block copolymer. The thermal stability of the block copolymer was lower than that of PU mainly due to the higher content of temperature susceptible PGAMA block in the block copolymer.

DSC thermograms of the HO-PU-OH, PGAMA and two block copolymers $PGAMA_6$-*b*-PU-*b*-$PGAMA_6$ and $PGAMA_{30}$-*b*-PU-*b*-$PGAMA_{30}$ are shown in Figure 8. The glass transition temperature (T_g) of HO-PU-OH was observed at approximately –40.9°C, while the melting temperatures (T_m) were observed at ~17.7°C with the corresponding heat of fusion (ΔH_m) of 32.5 J/g due to the melting of soft segment consisting of PTMG and at ~97.2°C with the corresponding ΔH_m of 1.2 J/g due to the hard segment consisting of HMDI from PU. The low intensity higher temperature peak is due to low abundance of hard segment content in the PU chain. It is worthy to mention that the T_g of PGAMA was observed at ~85.5°C. For the block copolymer $PGAMA_6$-*b*-PU-*b*-$PGAMA_6$, a very weak T_m of the semi-crystalline soft PTMG segment of the PU block was observed at ~9.6°C, while the T_m of the crystalline hard segment of the PU block was observed at ~88.3°C. This suppression of the T_g of the PU segment and the T_m of the PTMG block of the PU segment may be due to the miscibility of the melt PU segments with longer amorphous PGAMA segment through the formation of PU micro-domain in PGAMA macro-domain. There may be another possibility that the T_g of the amorphous PGAMA block may merge with the melting temperature of hard segment ~88°C. Similar DSC thermograms were also observed with the block copolymers $PGAMA_{30}$-*b*-PU-*b*-$PGAMA_{30}$ having longer PGAMA segments. So, all these observations supported the successful formation of PGAMA-*b*-PU-*b*-PGAMA block copolymers.

Controlled Synthesis of Ag-Nanoparticles

The usefulness of the typical amphiphilic block copolymers has been demonstrated for synthesizing nanoparticle with varying size. The change of color of the homogeneous mixture of $AgNO_3$ and $PGAMA_{30}$-*b*-PU-*b*-$PGAMA_{30}$ block copolymer in deionized water/DMF (9:1, v/v) mixture from colorless to reddish brown upon addition of the reducing agent $NaBH_4$ was indicative of the formation of silver nanoparticles. The appearance of a distinct characteristic absorption peak at ~421 nm in the UV-Vis spectrum [Figure 9(a)] confirms the existence of Ag nanoparticle.[42] Moreover, a strong absorbance peak at ~248 nm of pure block copolymer solution indicate its micellar structure while its disappearance/very diffused peak strongly suggest the breakage of micelles in presence of Ag ion. However, the Ag-nanoparticle colloids are stable in dispersion even after 1 year as evidenced by the absence of any precipitated/aggregated silver nanoparticles. Silver ion reduction was conducted with similar ion and polymer concentration but with varying block length of PGAMA. The red shifting of the distinct characteristic peak corresponds to silver nanoparticles has been observed in the UV-Vis spectra with increasing chain length of the PGAMA segment of the PGAMA-*b*-PU-*b*-PGAMA block copolymers [Figure 9(b)] clearly indicating the formation of larger Ag-nanoparticles using

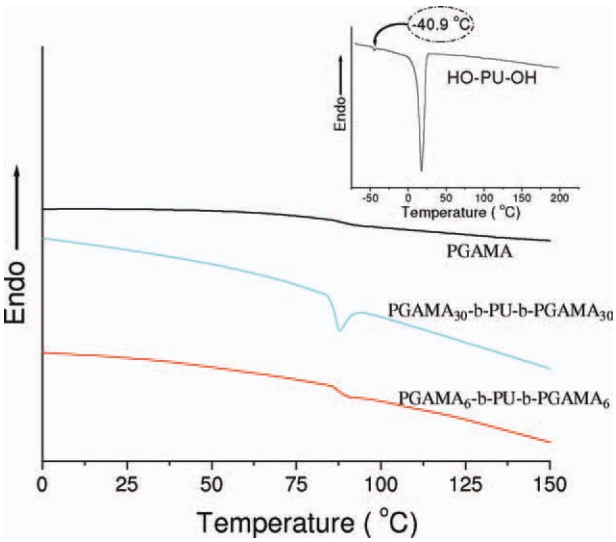

Figure 8. DSC thermograms of the HO-PU-OH, PGAMA, and two block copolymers $PGAMA_6$-*b*-PU-*b*-$PGAMA_6$, and $PGAMA_{30}$-*b*-PU-*b*-$PGAMA_{30}$. [Color figure can be viewed in the online issue, which is available at wileyonlinelibrary.com.]

Applied Polymer SCIENCE

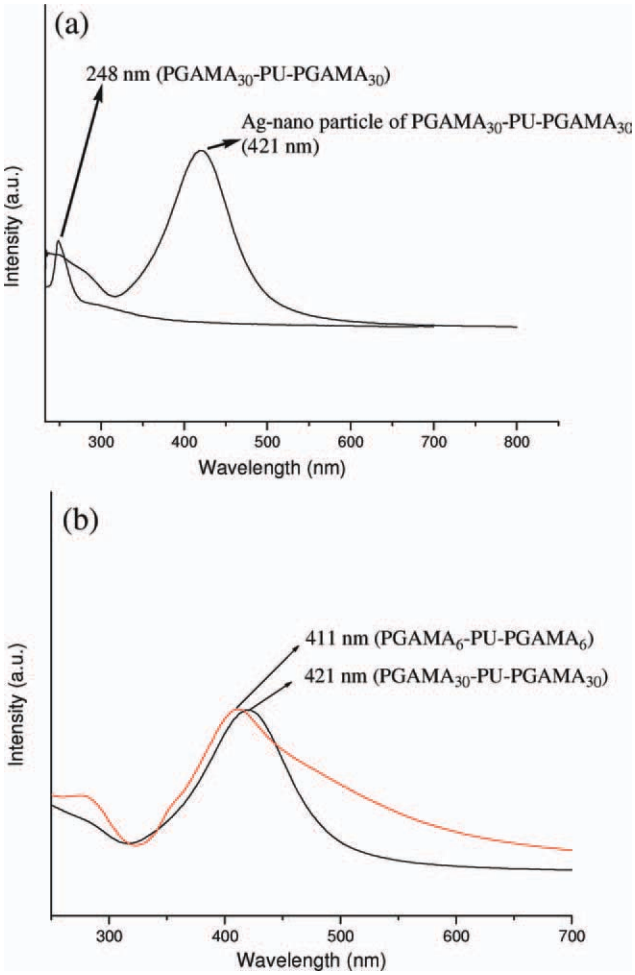

Figure 9. (a) UV-Vis spectra of Ag-nano-particles formed using $PGAMA_{30}$-*b*-PU-*b*-$PGAMA_{30}$ triblock copolymer and of the only block copolymer $PGAMA_{30}$-*b*-PU-*b*-$PGAMA_{30}$ in DMF/water (1:9, v/v). (b) UV-Vis spectra of Ag-nano particles formed using of $PGAMA_6$-*b*-PU-*b*-$PGAMA_6$ and $PGAMA_{30}$-*b*-PU-*b*-$PGAMA_{30}$ triblock copolymers in DMF/water (1:9, v/v). [Color figure can be viewed in the online issue, which is available at wileyonlinelibrary.com.]

longer hydrophilic PGAMA chain. Further, the prominent peak at 248 nm, characteristics of micellar structure, gradually vanishes with larger block length of PGAMA in the presence of Ag ion suggesting the existence of some micellar environment for smaller PGAMA block presumably due to poor complex forming ability of Ag ion with very few PGAMA segment. On the contrary, large PGAMA block can form complex with Ag ion and, thereby, can destroy the micellar organization as evidenced from the diffuse to disappearance of peak. However, the size and shape of the resulted nanoparticles have been examined by using TEM. Figure 10 shows the spherical morphology of nanoparticles with average particle diameter of 15 nm for larger PGAMA block ($PGAMA_{30}$-*b*-PU-*b*-$PGAMA_{30}$). The average diameter of the nanoparticles is 7 nm for smaller PGAMA block ($PGAMA_6$-*b*-PU-*b*-$PGAMA_6$). Hence, fine tuning of nanoparticle dimension is made possible through varying PGAMA block length. It is noteworthy to mention that the corresponding control reaction without using block copolymer showed the formation of the unstable aggregated black color Ag particles. In addition, there was a formation of unstable Ag particle flocculation using the same block copolymer at the concentration below its CMC value. This clearly suggests that the minimum polymer concentration is the precondition of metal nanoparticles synthesis as stable complexation can only be formed in presence of sufficiently lengthy chain through coordinate bonding. Further, the high resolution

TEM image distinctly show the planner spacing of 0.25 nm indicative of Ag crystal of (100) plane (inset image Figure 10). Moreover, the relative particle dimensions were confirmed by the DLS study of the corresponding Ag-nanoparticles (Supporting Information Table S1, Figures S1b and S1d). The absolute value of particle dimension differ in DLS presumably due to hydrodynamic volume of particles embedded in polymer chain in solution phase while TEM measurements have been performed after removing the solvent. Similar type of result was

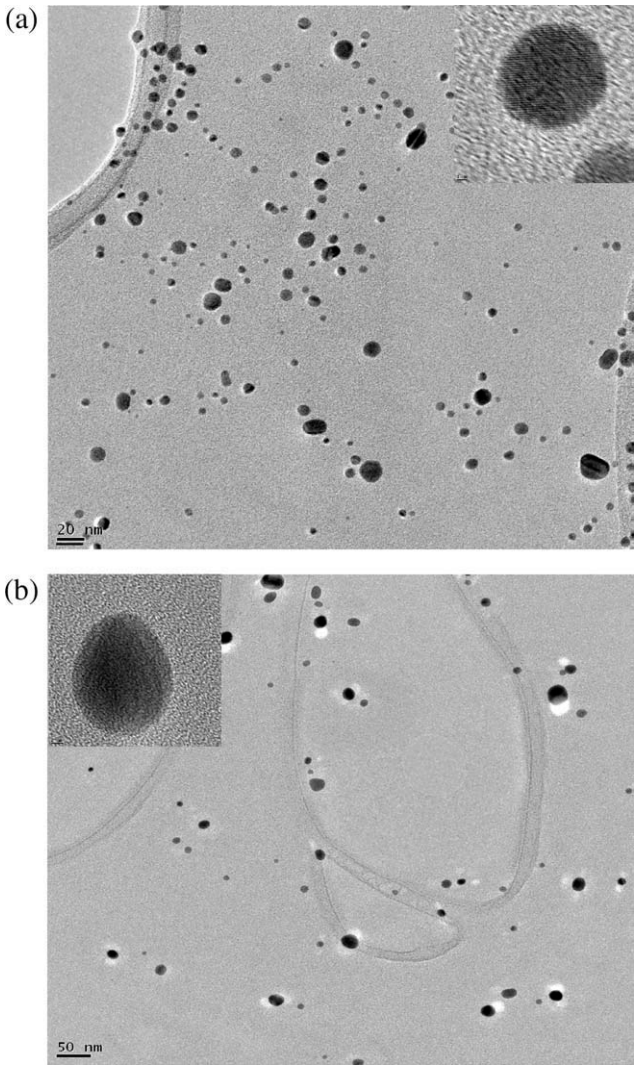

Figure 10. TEM images of Ag-nano particle obtained using (a) $PGAMA_6$-*b*-PU-*b*-$PGAMA_6$ and (b) $PGAMA_{30}$-*b*-PU-*b*-$PGAMA_{30}$ (high resolution TEM of single particle as inset in both images).

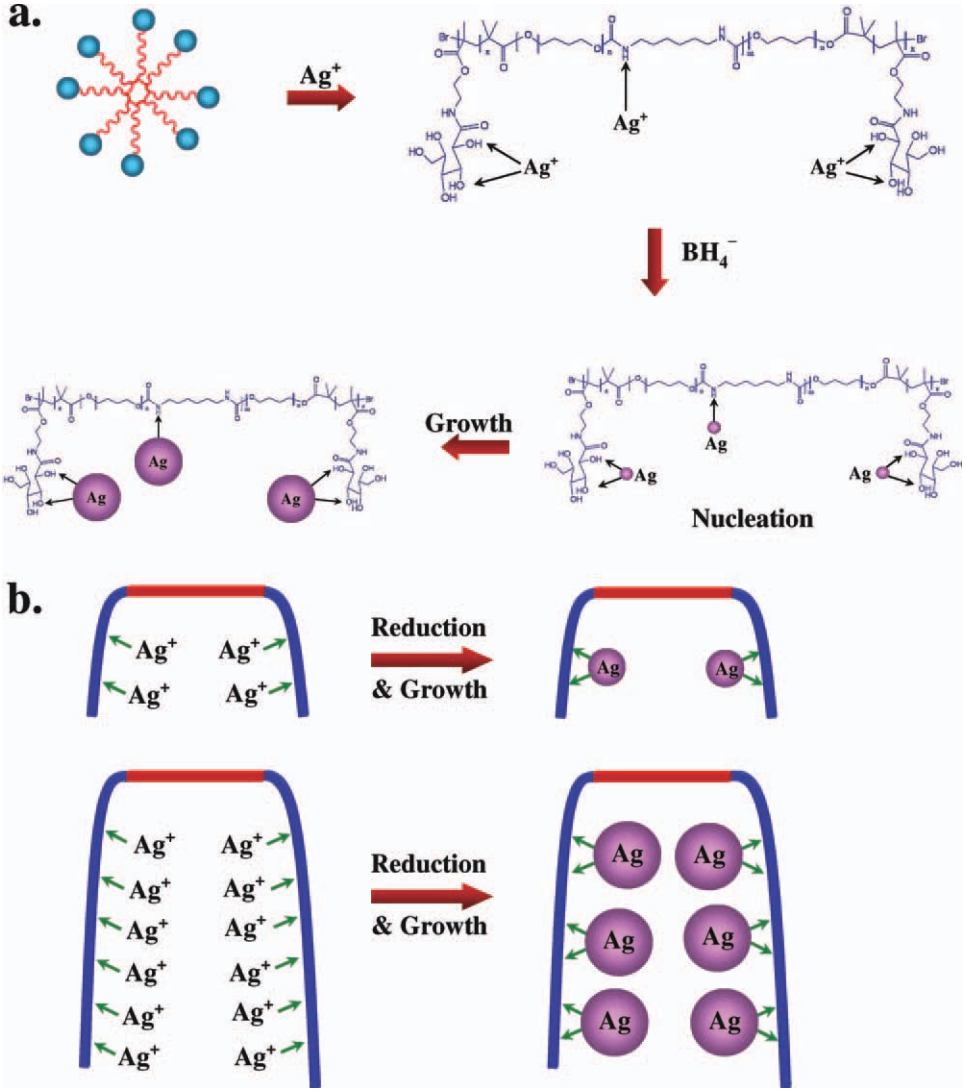

Scheme 3. Schematic representation of (a) formation of Ag nanoparticle and, (b) mechanistic approach of forming different particle dimension in different block length. [Color figure can be viewed in the online issue, which is available at wileyonlinelibrary.com.]

also reported for the synthesis of gold naoparticles using poly(-ethylene oxide)-*b*-poly(propylene oxide)-*b*-poly(ethylene oxide) amphiphilic PEO-PPO-PEO block copolymers.[43] Therefore, these triblock copolymers are very useful for the synthesis of regulated Ag-nanoparticles. More importantly, one can regulate the size of metal nanoparticles by varying the size of hydrophilic PGAMA chain length. Now, it is important to know the mechanism of nanoparticle synthesis and its controlled dimension by changing the block length. A scheme for the Ag-nanoparticle synthesis has been proposed: double hydrophilic PGAMA-*b*-PU-*b*-PGAMA block copolymers form micelles through the aggregation with the hydrophobic PU segments as the core and the hydrophilic PGAMA as the shell. Ag^+ ions can form complex preferably with the pendent hydroxyl group of PGAMA resulting the breakage of micellar structure in presence of Ag ions. Then, the reduction of Ag^+ to Ag takes place after addition of $NaBH_4$ and the metal gets stabilized within the hydrophilic pendant PGAMA cage through complexation followed by its growth to bigger size of Ag nanoparticles [Scheme 3(a)]. For a specific Ag^+ and $NaBH_4$ concentration, complexation of Ag^+ with the pendent hydroxyl group of the PGAMA chain is more efficient and high in number density for longer block size of hydrophilic PGAMA chain and during growth process few of those nuclei may merge forming larger nanoparticle [Scheme 3(b)]. On the contrary, for smaller block length like in $PGAMA_6$-*b*-PU-*b*-$PGAMA_6$ only few complexes can form leading to very few nucleation site and small particle can be stable in smaller dimension hydrophilic cage. Further, the size distribution of nanoparticles has also been explained in a similar manner with stabilization of nanoparticle point of view. In this regard, the formation of Ag nanoparticles within the medium cannot be ruled out and such Ag nanoparticles may get stabilized through the adsorption at the hydrophilic PGAMA region restricting their precipitation. However, the dimension of the Ag nanoparticle can be varied using different length of amphiphilic block of the copolymer.

CONCLUSIONS

In conclusion, novel amphiphilic ABA-type PGAMA-*b*-PU-*b*-PGAMA triblock copolymers were successfully synthesized by combining the step-growth and copper-catalyzed ATRP polymerizations. The resulting block copolymers formed spherical micelles in water as revealed by TEM, supported by ^{1}H-NMR spectroscopy, and light scattering. Miceller size increases with increase in hydrophilic PGAMA chain length as revealed by DLS study. The CMC value of the resulting block copolymers increased with the increase of the chain length of the PGAMA block. Thermal studies by TGA and DSC supported the block copolymer formation and their relative thermal stability and interaction. Spherical Ag-nanoparticles were successfully synthesized using these block copolymers as stabilizer and size of the Ag nanoparticles can be tailored by altering the length of amphiphilic chain length (PGAMA). Higher is the PGAMA length larger is the Ag nanoparticle. A complexation mechanism has been proposed for the formation of stable and regulated Ag nanoparticle using various chain length of hydrophilic PGAMA block of the tri-block copolymer. Synthesis of such amphiphilic block copolymers will find extensive applications in drug delivery and metal nanoparticle synthesis. Moreover, the Ag-nanocomposite of such block copolymer may find applications in antimicrobial coating and wound healing applications.

ACKNOWLEDGMENTS

The authors gratefully acknowledge the financial support from the Department of Science and Technology, Government of India, through grant no. SR/S1/PC-25/2006. NKV, VKP, and AKM acknowledge the Council of Scientific and Industrial Research (CSIR), Government of India for Research Fellowships. CSB acknowledges the University Grant Commission (UGC), Government of India for Research Fellowship. The authors also acknowledge the partial financial support from Banaras Hindu University.

REFERENCES

1. Ouchi, M.; Terashima, T.; Sawamoto, M. *Chem. Rev.* **2009,** *109*, 4963.
2. Yamago, S. *Chem. Rev.* **2009,** *109*, 5051.
3. Kedar, U.; Phutane, P.; Shidhaye, S.; Kadam, V. *Nanomed.: Nanotechnol. Biol. Med.* **2010,** *6*, 714.
4. Lee, H.; Lee, E.; Kim, D. K.; Jang, N. K.; Jeong, Y. Y.; Jon, S. *J. Am. Chem. Soc.* **2006,** *128*, 7383.
5. Chen, H.; Wu, X.; Duan, H.; Wang, Y. A.; Wang, L.; Zhang, M.; Mao, H. *ACS Appl. Mater. Interface* **2009,** *10*, 2134.
6. Shin, W.-J.; Basarir, F.; Yoon, T.-H.; Lee, J.-S. *Langmuir* **2009,** *25*, 3344.
7. Callewaert, M.; Gohy, J.-F.; Dupont-Gillain, C. C.; Petermann, L. B.; Rouxhet, P. G. *Surface Sci.* **2005,** *575*, 125.
8. Spatz, J. P.; Roescher, A.; Moller, M. *Adv. Mater.* **1996,** *8*, 337.
9. Liu, Y.; Tu, W.; Cao, D. *Ind. Eng. Chem. Res.* **2010,** *49*, 2707.
10. Sakai, T.; Alexandridis, P. *J. Phys. Chem. B* **2005,** *109*, 7766.
11. Perelstein, O. E.; Ivanov, V. A.; Moller, M.; Potemkin, I. I. *Macromolecules* **2010,** *43*, 5442.
12. Bulychev, N. A.; Arutunov, I. A.; Zubov, V. P.; Verdonck, B.; Zhang, T.; Goethals, E. J.; Du Prez, F. E. *Macromol. Chem. Phys.* **2004,** *205*, 2457.
13. Sakai, T.; Alexandridis, P. *Langmuir* **2004,** *20*, 8426.
14. Aryal, S.; Prabaharana, M.; Pilla, S.; Gong, S. *Int. J. Biol. Macromol.* **2009,** *44*, 346.
15. Signori, F.; Chiellini, F.; Solaro, R. *Polymer* **2005,** *46*, 9642.
16. Hu, Z.; Fan, X.; Wang, H.; Wang, J. *Polymer* **2009,** *50*, 4175.
17. Borges, M. R.; Santos, J. A.; Vieira, M.; Balaban, R. *Mater. Sci. Eng. C* **2009,** *29*, 519.
18. Narain, R. *React. Funct. Polym.* **2006,** *66*, 1589.
19. Lipinski, T.; Kitov, P. I.; Szpacenko, A.; Paszkiewicz, E.; Bundle, D. R. *Bioconjugate Chem.* **2011,** *22*, 274.
20. Ohno, K.; Tsujii, Y.; Fukuda, T. *J. Polym, Sci., Part A, Polym. Chem.* **1998,** *36*, 2473.
21. Chen, Y. M.; Wulff, G. *Macromol. Chem. Phys.* **2001,** *202*, 3273.
22. Chen, Y. M.; Wulff, G. *Macromol. Chem. Phys.* **2001,** *202*, 3426.
23. Chen, Y. M.; Wulff, G. *Macromol. Rapid Commun.* **2002,** *23*, 59.
24. Ejaz, M.; Ohno, K.; Tsujii, Y.; Fukuda, T. *Macromolecules* **2000,** *33*, 2870.
25. Narain, R.; Armes, S. P. *Chem. Commun.* **2002, 2776.**
26. Narain, R.; Armes, S. P. *Macromolecules* **2003,** *36*, 4675.
27. Narain, R.; Armes, S. P. *Biomacromolecules* **2003,** *4*, 1746.
28. Szycher, M. Szycher Handbook of Polyurethanes, CRC Press LLC: Florida, **1999.**
29. Sun, L.-N.; Yu, J.; Peng, H.; Zhang, J. Z.; Shi, L.-Y.; Wolfbeis, O. S. *J. Phys. Chem. C* **2010,** *114*, 12642.
30. Zhou, L.; Yu, L.; Ding, M.; Li, J.; Tan, H.; Wang, Z.; Fu, Q. *Macromolecules* **2011,** *44*, 857.
31. Verma, H.; Kannan, T. *Polym. Intl.* **2008,** *57*, 226.
32. Verma, H.; Kannan, T. *Polym. J.* **2008,** *40*, 867.
33. Verma, H.; Kannan, T. *Express Polym. Lett.* **2008,** *2*, 579.
34. Lan, P. N.; Corneillie, S.; Schacht, E.; Davies, M.; Shard, A. *Biomaterial* **1996,** *17*, 2273.
35. Nayak, S.; Verma, H.; Kannan, T. *Colloid Polym. Sci.* **2010,** *288*, 181.
36. Lutz, J.-F.; Neugebauer, D.; Matyjaszewski, K. *J. Am. Chem. Soc.* **2003,** *125*, 6986.
37. Mishra, A. K.; Patel, V. K.; Vishwakarma, N. K.; Biswas, C. S.; Raula, M.; Mishra, A.; Mandal, T. K.; Ray, B. *Macromolecules* **2011,** *44*, 2465.
38. Chen, Y.; Dong, C.-M. *J. Phys. Chem. B* **2010,** *114*, 7461.
39. Wang, Y.-C.; Tang, L.-Y.; Sun, T.-M.; Li, C.-H.; Xiong, M.-H.; Wang, J. *Biomacromolecules* **2008,** *9*, 388.
40. Wang, F.; Bronich, T. K.; Kabanov, A. V.; Rauh, R. D.; Roovers, J. *Bioconjugate Chem.* **2005,** *16*, 397.
41. Mishra, A., Aswal, V. K., and Maiti, P. *J. Phys. Chem.: B* **2010,** *114*, 5292.
42. Link, S.; El-Sayed, M. A. *J. Phys. Chem.: B* **1999,** *103*, 8410.
43. Sakai, T.; Alexandridis, P. *J. Phys. Chem.: B* **2005,** *109*, 7766.